PARTICLE CONTAMINATION IN VACUUM SYSTEMS

J Martignac, B.Bonin, C.Henriot, JP.Poupeau
CEA SACLAY, DSM/DAPNIA/SEA91191 GIF/YVETTE
I.Koltchakian, D.Kocic,Ch.Herbeaux, JP.Marx
LURE 91400 ORSAY

Abstract : Many vacuum devices, like RF cavities, are sensitive to particle contamination. This fact has motivated a considerable effort of cleanliness from the SRF community. The present paper reports the first results of a general study trying to identify the most contaminating steps during assembly and vacuum operation of the cavity. The steps investigated here are gasket assembly, evacuation and venting of the vacuum system, and operation of sputter ion pumps.

1- Introduction

It is well know that dust particles are terrible enemies of Superconducting Cavities [ref 1]. Recently, efforts have been made to improve the cavity cleaning techniques. Generalised use of automatized chemical treatment [ref 2] and high pressure rising facilities [ref 3] have improved considerably the cavity performance level. But this effort towards cleanliness can be spoiled if the next steps in the cavity life (assembly, and operation under vacuum) recontaminate its surface. It has been shown on a statistical basis that cavities having had trouble during assembly steps or vacuum operation, have a significantly lower field emission threshold and overall performance level [ref 4].
The risk of contamination during the cavity assembly and vacuum operation must be measured, and minimized. The present paper reports the first results of a general study intended to identify the most dangerous steps and components:

1. gasket assembly
2. valve operation
3. pre-pumping and venting
4. steady state pumping by ion-pumps and getters
5. particle liberation by walls under the influence of shocks or vibrations

The present paper will describe only results on items 1, 3 and 4. The main tools for this study are particle counters operating in air or under vacuum. The counters are placed close to the component or to the location of the suspected contamination during the abovementioned operations.

2- Particle counters description

Met-One 205 Model

This counter detects the number of particles contained in 28.3 liters air volume. This volume is pumped through a conic head sensor and then the particles are detected with a laser diode. The detected particle sizes are : 0.16, 0.2, 0.3, 0.5 ,1 and 5 µm.

HYT PM 250 Model

The HYT PM250 sensor can operate in air or in vacuum. The particles fall through a window crossing in its center a laser beam of about 1 mm diameter. Photodetectors receive the light scattered by the particles. The particle size is proportional to the intensity peak. The detected particle sizes are : 0.19, 0.27, 0.3, 0.4 and 0.5 µm.

Counter calibration

The two counters were used in the same gas flow in order to compare their coutings. The couting ratio K between both counters was not exactly the same for all particle sizes:

- 0.16 µm < X < 0.29 µm ⇨ K = 7
- 0.3 µm < X < 0.49 µm ⇨ K = 5.4
- All particle sizes ⇨ K = 6.2

From this last value, the sensitive area of detection of the PM250 counter was determinated: $S_{eff} \cong \frac{S_{window}}{6.2} = 0.4\ cm^2$

In the rest of this paper, the particle countings by the PM250 sensor can be transformed into particle fluxes by division by the effective area of detection: S_{eff}.

3- Particle contamination by gaskets setting

The particle contamination by the gasket setting was evaluated for conflat (CF35) and helicoflex gaskets.

This kind of measurement does not require a counter able to work under vacuum, so the Met-One sensor was used for convenience. The sensor was installed directly downstream the tested gasket (fig: 3.1). Due to the flow aspiration, it can resonably be assumed that all generated particles are detected. The experiment was conducted in a clean room class 100, by trained operators. All components were washed with 18 MΩ deionised water prior to assembly.

For the tests we used a particular process which is as follow:

1. Installation of a cleaned joint
2. Installation of a cleaned flange
3. Installation of the cleaned screws on the top of the flange
4. Installation of the cleaned nuts and washers
5. Tightening without moving the screws

Experimental device :

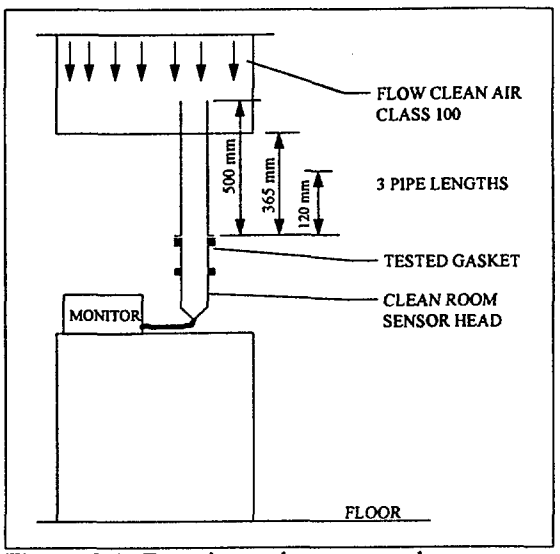

Figure 3.1: Experimental set-up used to measure the particle contamination during CF or Helicoflex setting.

Results :

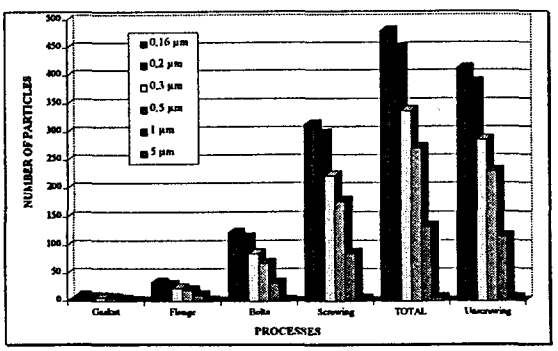

Diagram 1 : Setting of a CF35 flange - Average on 10 gaskets - Pipe of 120 mm. long.

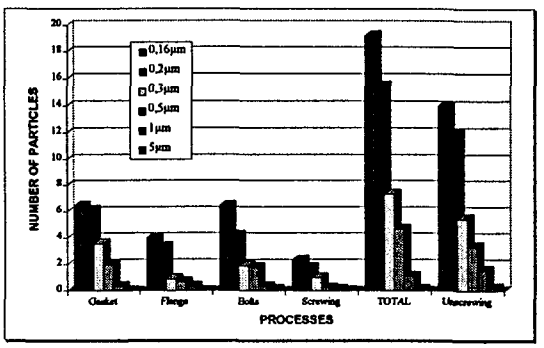

Diagram 2 : Setting of the CF35 flanges Average on 10 gaskets - Pipe of 500 mm. long.

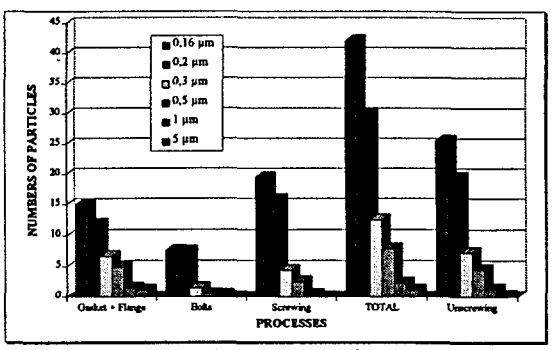

Diagram 3 : Setting of the flanges with an Helicoflex gasket (n°:15040) - Average on 8 gaskets - Pipe of 365 mm. long

The standard deviation S results, on 10 measurements for all the processes are as follow:

Diagram 1 : S = 180 for m* = 480
Diagram 2 : S = 16 for m* = 19
Diagram 3 : S = 18 for m* = 42
(* : m = average)

Conclusion

- Gasket assembly is contaminating;
- There is no clear influence of the nature of the gasket;
- No particles are liberated between assembly steps, this particle generation is due to the operator. Some of the particles are of human origin (this contribution is smaller if the pipe is higher); some particles may also be liberated by shocks or vibrations during the assembly.

4- Particle contamination by Sputter-Ion pump

The sputter-ion pump tested was a Varian Vacion Plus 75 StarCell. The PM250 sensor was placed just below the pump for a better sensitivity (fig 4.1).

As can be seen in fig 4.2, the pump in normal operation ($p < 10^{-4}$ Pa) does not generate particles since the measured contamination level (1.42 particles/min) is almost the same as the detector background noise (1.25 particles/min). The only particle generation observed occurs during startup ($p \approx 10^{-3}$ Pa.). Some particles bursts (about 10 particles) are also observed during arcing. Of course, the ion-pump can also liberate particles because of shocks or vibrations, like any vacuum chamber wall. These contributions can be minimized if the pump is operated in vertical position, with the flange on the top.

Experimental device :

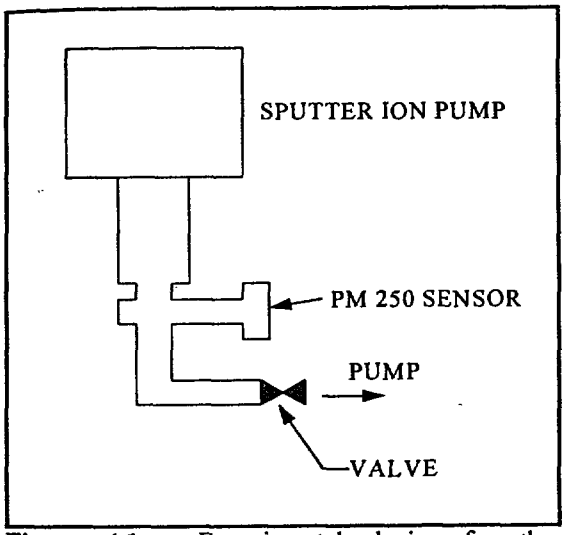

Figure 4.1 : Experimental device for the measurement of the dust contamination by the sputter-ion pump.

Results :

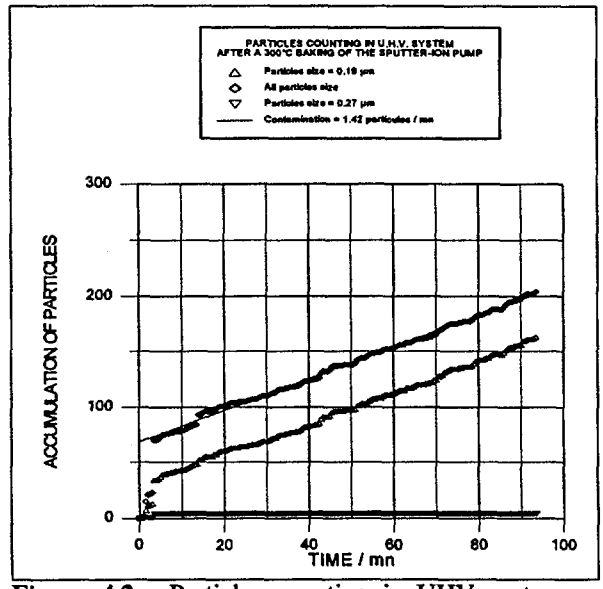

Figure 4.2 : Particles counting in UHV system after a 300°C baking of the sputter-ion pump

Generally, the particle sizes distribution is as follows :

- ≈ 50 % [0.19 µm ; 0.27 µm[
- ≈ 10 % [0.27 µm ; 0.3 µm[
- ≈ 15 % [0.3 µm ; 0.4 µm[
- ≈ 10 % [0.4 µm ; 0.5 µm[
- ≈ 15 % ≥0.5 µm

5- Contamination during pre-pumping and venting operations

Evacuation or venting of the cavity are also potentially contaminating steps because turbulent gas flow can release and transport particles. To evaluate this contamination we used an experimental device shown in fig 5.1. For pre-pumping , the regulation valve V_1 was closed; for venting V_1 was opened.

This experiment showed that the particle generation is observed mainly at the beginning of the evacuation process, and practically stops when the vacuum level becomes lower than 5.10^4 Pa . A smaller number of particles is generated if the evacuation is slower.

Particle generation during venting is also very significant, specially at the beginning of the process. Here, the opening of valve V_1 determines the speed of the venting. The influence of this speed on particle generation has not yet been examined in detail.

As will be justified in the next paragraph, particles are likely to be generated at the level of the valve V_1 itself, where the air speed and turbulence is largest. Reduction of the opening of V_1 reduces the air flow, but not the air speed at

V_1, and this might explain why particles are always generated during venting. The only plausible remedy we propose against this contamination is a filter located between V_1 and the vacuum vessel.

We have noticed also, when we pumped quickly, a formation of water droplets which can be eliminated with a 60°C baking of the vacuum vessel (fig 5.2). The difference between the percentage of the 0.5 µm particles for the experiment at 20 °C and for the experiment at 60 °C proves that the biggest particles are water droplets.

Experimental device :

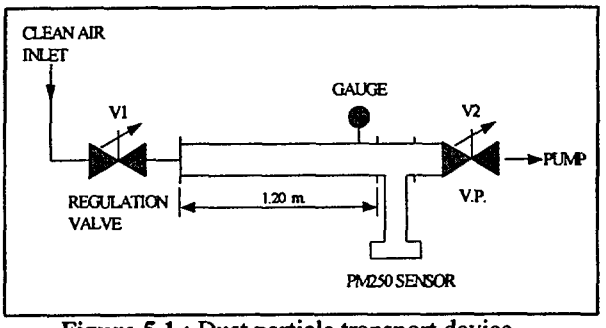

Figure 5.1 : Dust particle transport device

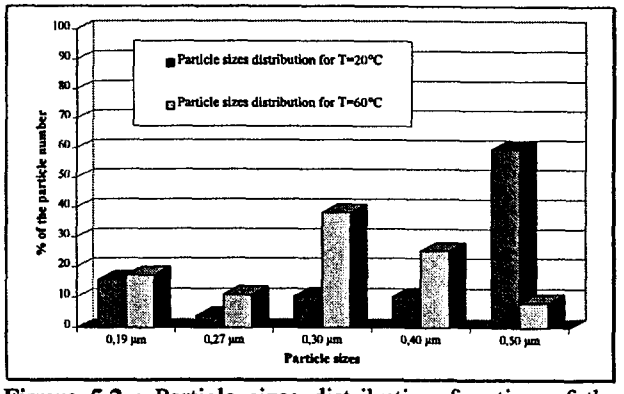

Figure 5.2 : Particle sizes distribution function of the operating temperature. Regulation valve is closed, V_2 is opened suddenly.

6- Contaminaton induced by the flow speed

In order to investigate this contamination, clean air coming from a class 100 laminar flow was pumped through a 1.20 m. long DN 40 pipe, with an adjustable flow rate (fig 6.1). The flow rate was controlled by a diaphragm at the upper end of the pipe, and by a regulation valve located close to the pump.

The source of the observed particles is probably the diaphragm, where the air speed is highest. As can be seen from fig 6.2 and 6.3, the relevant variable is not the flow rate, but the flow speed, which should be kept below 2 $m.s^{-1}$ at the diaphragm location for a particle-free operation. Note that the threshold between laminar and turbulent flow in the vicinity of the diaphragm occurs for flow speeds of about 2 $m.s^{-1}$. It is then tempting to correlate the onset of particle generation with the onset of turbulence. Further experiments will be undertaken to confirm this hypothesis, but we can already say that evacuation and venting of the cavity or vacuum vessel are contaminating steps, unless the flow is kept slow and / or laminar during these operations. This constraint applies not only at the cavity level, but also everywhere in the duct, including the narrowest sections, since the particles generated there can be transported on long distances (1.2 meters in our experiment).

Experimental device :

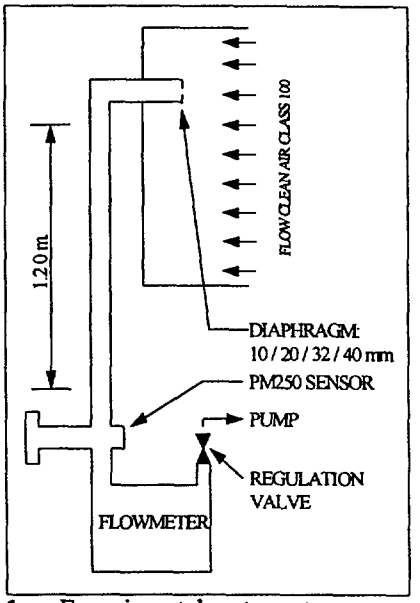

Figure 6.1 : Experimental set-up to measure the particle contamination induced by the flow speed.

Results :

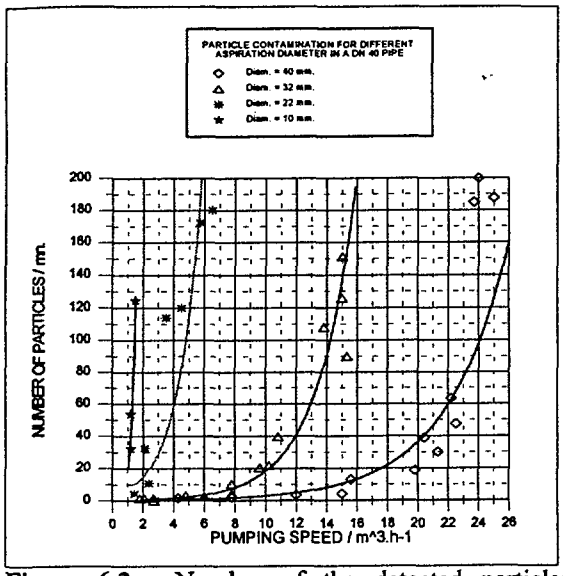

Figure 6.2 : Number of the detected particles (0.19µm < size < 0.5µm) as a function of the pumping speed.

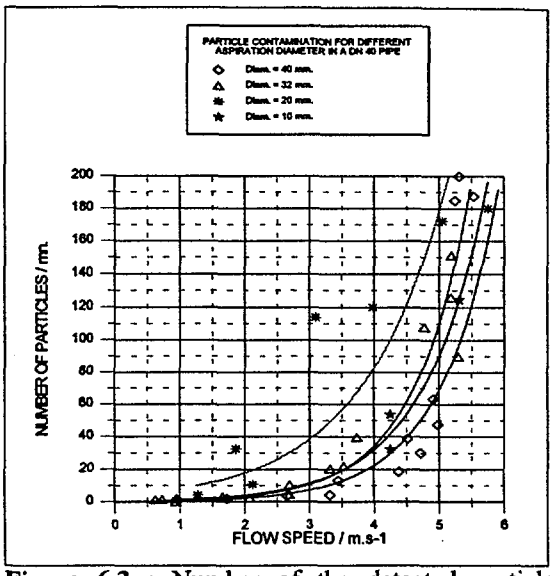

Figure 6.3 : Number of the detected particle (0.19µm < size < 0.5µm) as a function of the flow speed.

Acknowledgments

This work was supported by the S.E.A.(Service d'Etude des Accélérateurs), the vacuum group of LURE and the E.S.R.F.(European Synchrotron Radiation Facility). We thank F. Tardif from CEA/LETI for lending us an early version of vacuum particle counter.

References

[ref 1] : " High Voltage Vacuum Insulation " Acad. Press (1995) R.V. LATHAM, ed.

[ref 2] : " Dust contamination during chemical traitement of RF cavities : Symptoms and cures"
C.Z. Antoine et al, 5th Workshop on RF superconductivity, Hamburg' (1991), p. 456

[ref 3] : HP rinsing
D. BLOESS, Private communication;
P. KNEISEL et al
6th Workshop on RF superconductivity, CEBAF (1993), p. 628

[ref 4] : " A statistical analysis of the risk of dust contamination during assembly of RF superconducting cavities "
C. Antoine, 6th Worshop on RF superconductivity, CEBAF (1993), p. 1047

Measurements of the Anomalous RF Surface Resistance of Niobium Using a Dielectric Resonator

D. Moffat, M. Boloré, B. Bonin, E. Jacques, H. Safa
C.E. Saclay, DAPNIA/SEA, 91191 Gif sur Yvette Cedex, FRANCE

Abstract

The surface resistance of high and low RRR niobium plates at 4.2K and 1.8K has been measured as a function of many processing and testing parameters. A dielectric resonator was used instead of a resonant cavity. This resonator offered the ability to make many, sensitive measurements with an efficient use of time and helium. It was found that the surface resistance, R_S, of RRR = 190 niobium increased noticeably from the theoretical value if the cooling rate was slower than ~10 K/min. Fast-cooled plates subsequently warmed to 130K, and then recooled, showed a larger increase in R_S than plates warmed to either 100K or 160K. Both chemically polished, and electropolished RRR = 190 plates showed the effects of the "Q-virus". A heat treatment of 200°C made the RRR = 190 plates less susceptible to the "Q-virus". RRR = 30 niobium plates did not show any increase in R_S, regardless of treatment.

1. INTRODUCTION

Experiments have shown that the Q_0 of a niobium superconducting cavity may degrade if it is held in a certain temperature range immediately prior to testing. Saito and Kneisel [1] have determined that the dangerous temperature region lies between 70K and 150K, with the worst temperature being ~110K. It was found that the Q_0 of a cavity degraded monotonically with increasing hold time at 100K, for times as long as 25 hours. A saturation of the degradation was not observed. When the cavity was warmed above 200K and then quickly cooled to 4.2K, the degradation was completely eliminated. Additional results were presented in [2]. There have been anecdotal inferences that only high RRR niobium displays this Q_0 degradation.

Values of Q_0 of degraded cavities have been measured as a function of temperature and field below 4.2K [2, 3]. The temperature dependence found was not the expected BCS dependence. In addition, a change in slope was observed at ~2.2K. It was found that the Q_0 of a degraded cavity dropped abruptly at a particular field level (e.g. ~6 mT) when tested in this temperature regime [2, 3]. This behavior was reversible in field. No such effect was observed during testing of degraded cavities at 4.2K. These results were taken to indicate the presence of a superconducting-normal transition in some part of the cavity surface.

Only the layer of material within a penetration depth of the RF surface of a cavity affects its properties. This layer is extremely thin, on the order of tens of nanometers. Surprisingly, hydrogen has been found to be concentrated at niobium surfaces [4, 5] and a low-temperature phase transformation involving hydrogen is possible [6]. These facts have lead all investigators to conclude that hydrogen contamination is at the source of this phenomenon.

Many different laboratories have investigated the factors affecting the RF surface resistance, R_S, of niobium at 4.2K and lower (R_S is inversely proportional to Q_0). However, because measurements, materials, procedures, etc. vary widely, it has been difficult to draw specific conclusions as to which processing factors have the strongest influence on R_S. In this study we have applied a new measurement technique to this problem and have made many measurements in an attempt to determine the relative importance of the factors which influence what has been "affectionately" called the "Q-virus".

2. THE DIELECTRIC RESONATOR

For our investigation of this effect, we have chosen a different type of cavity, the dielectric resonator. A schematic of this resonator is shown in Figure 1. This

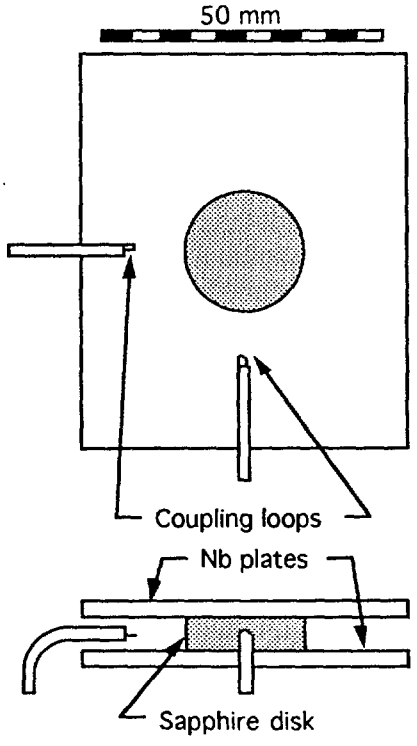

Figure 1. Schematic of the dielectric resonator. The coupling loops can be adjusted before testing. The clamp and carbon resistors have been omitted for clarity. The resonator is completely immersed in liquid helium during testing.

resonator is simple, inexpensive to operate, and has a fast turn-around time. The single-crystal sapphire disk is 21 mm in diameter and 6 mm tall. Loop couplers are used to excite the resonator and to measure its response. An aluminum frame with an adjusting screw holds everything together. A resistance heater is attached to the aluminum clamp. A carbon resistor is taped to each niobium plate to monitor their temperatures.

There are several choices to be made when using a resonator such as this -- operating mode, frequency, sapphire thickness, etc. TE modes were chosen for excitation because there are no E fields at the niobium/sapphire interfaces in these modes, making the Q_o measurements insensitive to helium films at these interfaces. The sapphire dimensions were chosen to produce a low resonant frequency while minimizing the dielectric losses.

Data were obtained with an HP 8510A network analyzer. The loaded Q value was determined by measuring Δf at the -3dB points on the transmitted power. The external Q's, and the unloaded Q_o, are determined using the following equations:

$$\alpha_{inc} = \frac{1 \pm 10^{-\Delta R/20}}{2} = \frac{Q_L}{Q_{inc}} \qquad (1)$$

$$\alpha_{trans} = \frac{10^{-T/10}}{4\alpha_{inc}} = \frac{Q_L}{Q_{trans}} \qquad (2)$$

$$\alpha_o = 1 - \alpha_{inc} - \alpha_{trans} = \frac{Q_L}{Q_o} \qquad (3)$$

where ΔR is the drop, in dB, of the reflected signal at the resonance and T is the absolute transmitted power at the resonance. Because T is an absolute measurement, the cable attenuations must be measured at the frequencies of interest. To verify the calculations of Q_{trans}, which depends on the value of α_{inc}, the cables were reversed and Q_{trans} was measured directly. The calculations and the measurements were always in close agreement. Typically, the external Q's were 4-5 x 10^7 for the incident coupler, 8-10 x 10^7 for the transmitted coupler.

Unloaded Q_o's were measured in two different modes: the TE_{011} and the TE_{012}. The frequencies of these modes are ~9.52 and 12.25 GHz, respectively. It was expected that the TE_{012} mode would be more sensitive than the TE_{011} mode to the surface roughness of the niobium plates. This was found to be true. For this reason, only the results from the TE_{011} mode will be presented and discussed.

The data will be presented in terms of the surface resistance of the niobium plates as this is a quantity of more general interest. This is obtained using:

$$R_s = \frac{G}{Q_o} \qquad (4)$$

where G is the "geometry factor" for the mode of interest -- 294 Ω for the TE_{011} mode, 602 Ω for the TE_{012} mode.

This resonator rests in a liquid helium bath, i.e. liquid helium is part of the resonator. While the losses of the helium are low and are not believed to affect the Q measurements, we have noticed interesting effects of the bath temperature on frequency (Figure 2).

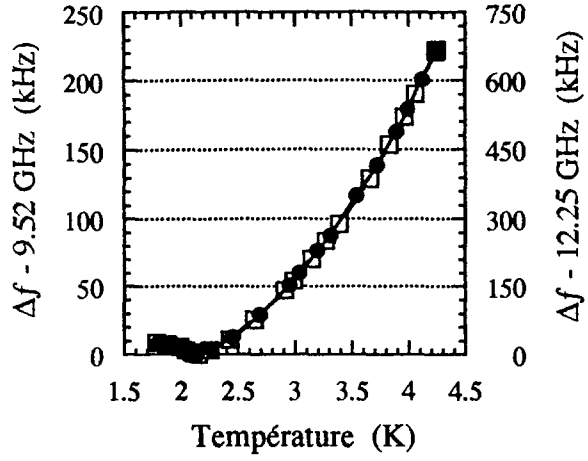

Figure 2. Temperature dependence of the resonance frequencies. The filled symbols correspond to the 9.52 GHz mode. The frequency differences for each mode are calculated relative to the frequency at 2.2K.

The resonator was cooled from room temperature many times during the course of this investigation. Figure 3 shows the measurements made on three different pairs of plates under the same cooling conditions. These data show that this resonator produces reproducible results with an absolute error bar of ±5μΩ at 9.52 GHz.

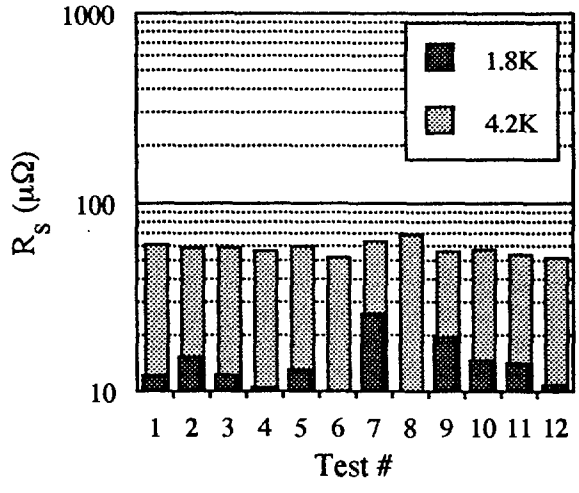

Figure 3. The results of twelve different measurements of surface resistance. The resonator was cooled quickly from room temperature for each test. All measurements were made at 9.52 GHz. Tests 1-5 used chemically polished, high RRR plates. Tests 6-8 used chemically polished, low RRR plates. Tests 9-12 used electropolished, high RRR plates. R_s at 1.8K was not measured in tests 6 and 8.

3. SAMPLE PREPARATION

Three different pairs of plates were used in the present study. The RF surfaces of all plates were milled using standard machining techniques and lubricants. This

produced a flat surface over the entire plate. The surface roughness of the machined surface was reduced using 320 grit abrasive paper. The plates were then ultrasonically degreased.

All plates received some form of chemical attack. One pair of plates was prepared from 3mm thick, high RRR, ~190, niobium and received a chemical polish using a 1:1:2 mixture of $HF:HNO_3:H_3PO_4$. (N.B. European HF is only 40%, in contrast to the American 48%). Approximately 60 μm were removed from the RF surfaces. A second pair of high RRR plates was electropolished after machining. The third pair of plates was prepared from 5mm thick, low RRR, ~30, niobium. Sixty four microns were removed from the RF surfaces of these plates using a 112 chemical polish.

4. EFFECT OF COOLING RATE

The RRR = 190, chemically polished plates were cooled from room temperature to 4.2K at four different cooling rates. The temperatures of the top and bottom plates were always within 5K of each other.

The results are shown in Figure 4. The values of R_S for the two fastest cooling rates are in good agreement with the BCS predictions. For the slower cooling rates, a noticeable increase in the surface resistance was seen. When the plates were cooled at 0.65K/min, R_S at 4.2K increased a factor of 3.1 above the BCS value, whereas at 1.8K it increased a factor of 6.6.

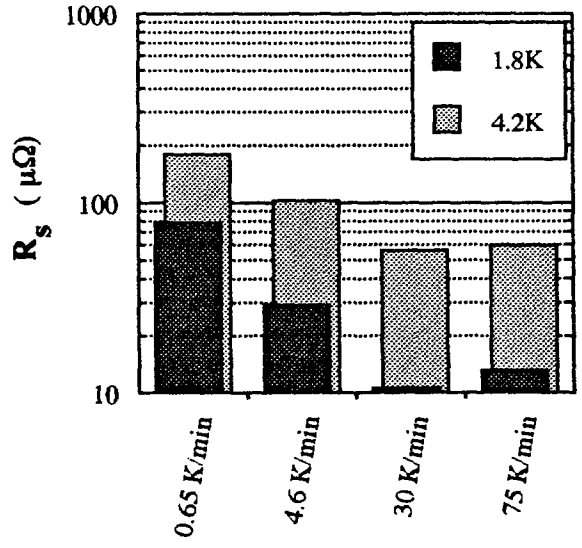

Figure 4. Effect of cooling rate on the surface resistance of RRR = 190 niobium at 9.52 GHz. The plates were cooled directly from room temperature to 4.2K.

5. EFFECT OF HOLDING TEMPERATURE

A typical thermal cycle for a resonator test is shown in Figure 5. The resonator was first cooled to 4.2K at a rate of ~60K/min. Measurements of R_S were made at 4.2K, while the helium bath was pumped to

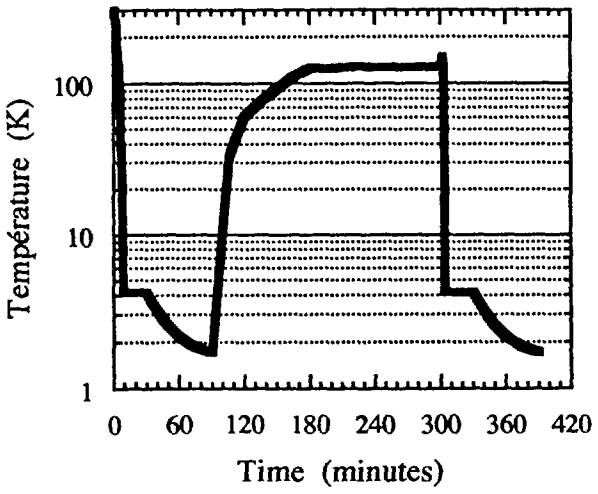

Figure 5. Typical thermal cycle of the dielectric resonator.

1.8K, and at 1.8K. These measurements established reference values for R_S. After all helium-temperature measurements were completed, the resonator was warmed to the chosen intermediate temperature, and held there, ± 5K, for ~2 hours. The resonator was then rapidly cooled to 4.2K again and the measurements repeated. After the second cooldown to 1.8K the resonator was warmed to room temperature over a period of ~12 hours. The results are shown in Figures 6, 7 and 8.

These data show that the holding temperature required to produce the greatest increase in R_S, at least at 9.52 GHz, is closer to 130K, rather than 100K. For a holding temperature of 130K, the electropolished plates showed a 3-fold increase in R_S at 4.2K, 4.5-fold at 1.8K. The effect was much more pronounced for the chemically polished plates -- R_S increased 15 times above the reference value at 4.2K, 44 times at 1.8K. In one or two tests R_S increased so much that it was difficult to identify the resonance.

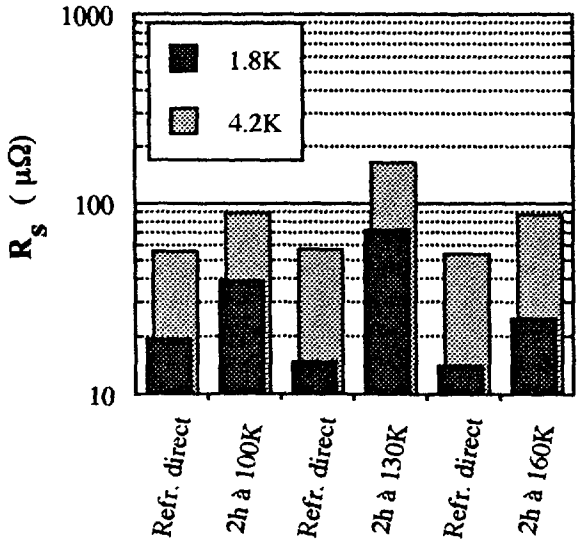

Figure 6. Effect of intermediate holding temperature on R_S for RRR = 190, electropolished plates. The thermal cycle shown in Figure 5 was used for each pair of measurements. Measurements were made at 9.52 GHz.

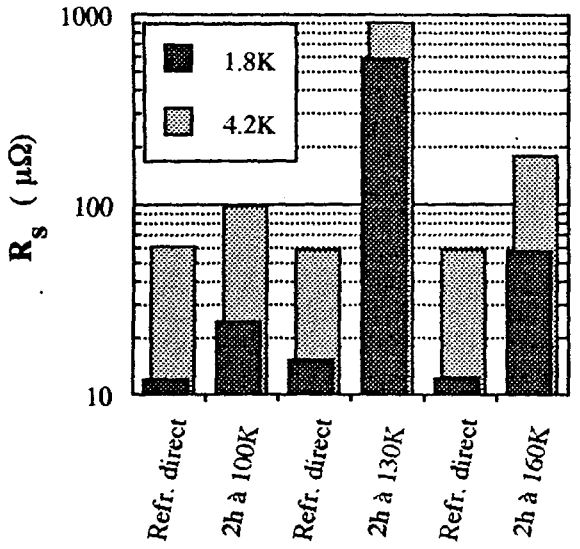

Figure 7. Effect of intermediate holding temperature on R_s for RRR = 190, chemically polished plates. The thermal cycle shown in Figure 5 was used for each pair of measurements. Measurements were made at 9.52 GHz.

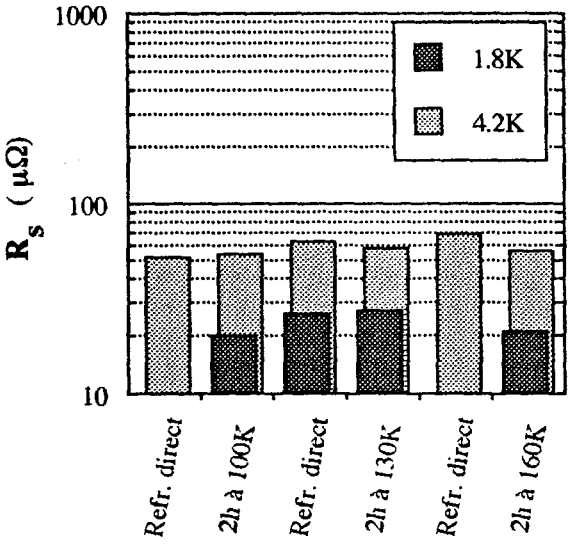

Figure 8. Effect of intermediate holding temperature on R_s for RRR = 30, chemically polished plates. The thermal cycle shown in Figure 5 was used for each pair of measurements. R_s at 1.8 was not measured for the first and fifth tests shown. Measurements were made at 9.52 GHz.

The data shown in Figure 8 clearly show that RRR = 30 niobium does not appear to be affected by the "Q-virus". That not even a slight effect was observed was surprising.

6. EFFECT OF 200°C HEAT TREATMENT

It is well known that a UHV heat treatment at 700 - 900°C will remove hydrogen from niobium and thus "inoculate" a cavity from the "Q-virus". The Nb-H phase diagram [6] shows that there is no stable hydride above 171°C. If a room temperature surface hydride were the cause of the "Q-virus", dissolving the hydride and diffusing the hydrogen into the bulk at some temperature between 171°C and 700°C may also "inoculate" a cavity.

The RRR = 190, chemically polished plates used to generate the data in Figure 7 were vacuum heat treated at 200°C for approximately two hours. The results are shown in Figure 9. This heat treatment produced no change in the reference values of R_s and was successful in reducing the effects of the "Q-virus". After a 200°C heat treatment, the increase in R_s after a 130K hold was only a factor of 3.6 at 4.2K, 3.8 at 1.8K.

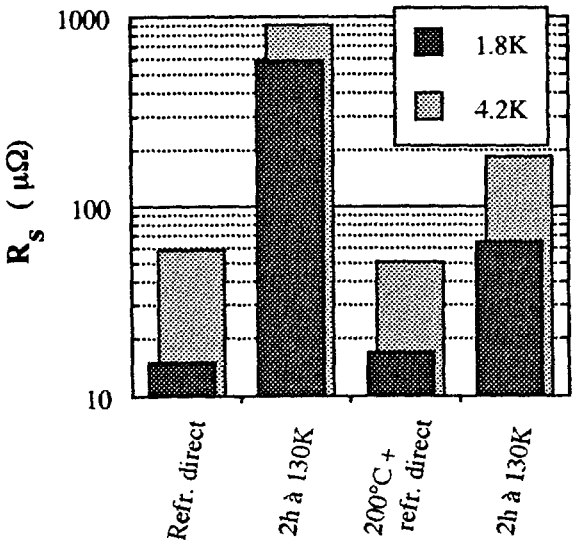

Figure 9. Effect of intermediate holding temperature on R_s for RRR = 190, chemically polished plates. The plates used to generate the data in Figure 7 were vacuum heat treated at 200°C for ~2 hours. Measurements were made at 9.52 GHz.

The RRR = 190, electropolished plates were also heat treated at 200 and 300°C. The surface resistance of these plates showed a factor of 2 improvement after the 200°C heat treatment, but were unchanged after a subsequent 300°C treatment.

7. EFFECT OF COLD-WORK

The metallurgical state of as-received niobium sheet is a quantity which is poorly defined and difficult to measure. It is possible that the degree of residual cold-work in high RRR niobium sheets is different than that in low RRR sheets. If so, this could have an effect on the hydrogen absorption properties of the sheets.

As a first attempt to study the influence of cold-work on the "Q-virus", two 5mm thick, RRR = 30 plates were tested in the as-received state. The results from these plates were shown in Figure 8. These plates were then rolled to 3mm in thickness, a cross-sectional area reduction of 40%. They were machined flat, and chemically polished again. Approximately 60 μm were removed from the RF surface during polishing.

The results of the tests are shown in Figure 10. One can see that the additional cold-work did not cause the "Q-virus" to appear in RRR = 30 niobium.

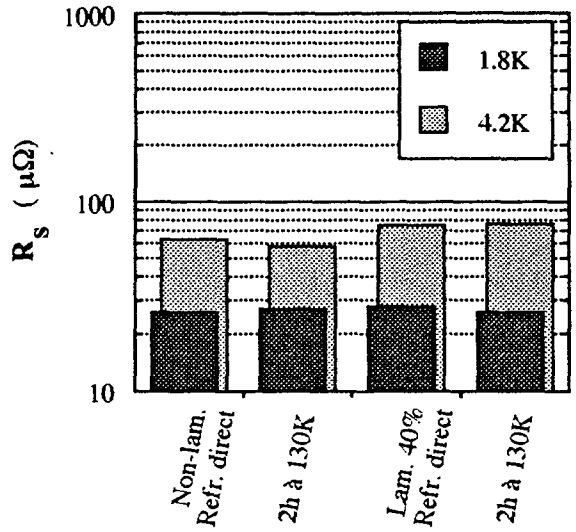

Figure 10. Effect of cold-work on R_s for RRR = 30 plates. The plates were tested at 5 mm thickness, then rolled to 3 mm thickness and tested again. The plates were chemically polished before each series of tests.

8. DISCUSSION

It has now been well demonstrated that the dielectric resonator is an effective tool for investigating the processing parameters which may affect R_S. The samples are easy and inexpensive to prepare, and testing is time and helium efficient.

The resonator made it possible to test the effect of cooling rate on R_S, something difficult to do with an accelerating cavity. It was found that rather fast cooling rates are necessary to achieve the theoretical R_S. This sensitivity to cooling rate may pose a problem for large accelerator modules.

The effect of hold temperature on R_S was roughly the same as measured by Saito and Kneisel. However, the temperature which produced the maximum degradation was somewhat higher in this study. This may be an artifact of the different test frequencies. It was also found that chemically polished plates were more sensitive to R_S degradation than electropolished plates. Perhaps this was due to the electropolishing technique.

The 200°C heat treatment was successful in reducing the effects of the "Q-virus". This demonstrates that it is not necessary to completely remove hydrogen from the walls of a cavity, only to displace it from the RF surface. The low temperature of this heat treatment may allow it to be applied to a cryostat when the effects of the "Q-virus" prove debilitating.

It has now been clearly shown that RRR = 30 niobium does not suffer from the "Q-virus" in the same manner as RRR = 190 niobium. Several more experiments need to be performed in order to fully understand why this is so. If high RRR niobium is contaminated or heavily cold-worked, does it become immune to the "Q-virus"? If low RRR niobium is purified, does it become susceptible to infection? If low RRR niobium is thoroughly annealed, but not purified, does it demonstrate the effects of the "Q-virus"?

At this point it is worthwhile to comment on three other incidental aspects of the present investigation. When comparing measured values of R_S as a function of temperature (between 4.2K and 1.8K) with the BCS values, we found that the agreement was quite good for tests with rapid cooling. However, when the resonator was cooled slowly, significant deviations were observed.

The R_S vs. temperature data were smooth and continuous, regardless of the thermal history of the resonator. Because the helium bath was part of the resonant circuit, bubbles, ice crystals, etc. in the helium caused some noise in the RF signal when the bath was above the λ point. For this reason, it was easier to record data while warming the resonator from 1.8K, rather than during pumping from 4.2K. When this was done, a significant change in R_S was observed at 2.2K. Further investigation showed that this was strictly an artifact caused by stratification in the helium. It is, therefore, presently believed that the previous evidence for a superconducting/ normal phase transformation at this temperature was also a result of stratification.

All measurements were made at two power levels in an attempt to observe a field dependence of R_S. No effect was seen although it should be noted that the maximum power output of the network analyzer was probably insufficient to observe this effect.

ACKNOWLEDGMENTS

One of us, D. Moffat, would like to thank the members of DAPNIA/SEA for their exceptional hospitality and camaraderie during his sabbatical visit. He would particularly like to thank B. Bonin for making the arrangements which made this visit a reality. The many discussions with, and tutoring in French by, C. Antoine were greatly appreciated.

REFERENCES

[1] K. Saito and P. Kneisel, *Proc. 3rd European Particle Accelerator Conference*, March 24-28, 1992, Berlin, Germany, 1231.

[2] J. Halbritter, P. Kneisel and K. Saito, *Proc. 6th Workshop on RF Superconductivity*, October 4-8, 1993, Newport News, VA, USA, 617.

[3] B. Bonin and R. Röth, *Particle Accelerators, 40*, 59 (1992).

[4] C. Antoine, et al., *Proc. 5th Workshop on RF Superconductivity*, August , 1991, Hamburg, Germany, 616.

[5] V. Nguyen-Tuong and L. Doolittle, *Proc. 6th Workshop on RF Superconductivity*, October 4-8, 1993, Newport News, VA, USA, 596.

[6] J. Smith, *Bull. Alloy Phase Diagrams, 4*(1), 1983.